

<sup>1</sup>Pavana H<sup>2</sup>Rohini Deshpande

## Design of Magnetic Field Harvester with Energy Management Unit to Power Sensors in Smart grid



**Abstract:** - Wireless sensors are used to implement monitoring of electrical devices in smart grid. Monitoring provides reliable power transfer and avoids cascading power failures. A dumbbell shaped magnetic core is developed and optimized to harvest electromagnetic field near bus bars and transformers in electrical substation. The energy thus harvested is used to power wireless sensors and make them self-sustainable. The experimental results show that the proposed core can harvest 1.25mW of output power with 2000 turns when placed in flux density of  $9\mu\text{T}$ rms. The power density is  $1.99\mu\text{W}/\text{cm}^3$ . Voltage doubler and energy management unit is designed to supply constant power to wireless sensors.

**Keywords:** Energy Management Unit, Smart grid, Electromagnetic field harvester, Wireless Sensors.

### I. INTRODUCTION

Power grid delivers power from producers to customers. In recent years electricity providers are implementing real time monitoring of voltage devices and transmission lines to avoid breakdowns and to ensure reliable operation by monitoring the operating conditions, wear and tear of the device [1]. Wireless Sensors is used to monitor the high voltage devices and power lines in real time. Wireless sensors have gained importance due to low power consumption and easy installation in locations that are hard to access. Wireless sensors are installed in power grid to measure voltage, current, temperature and partial discharge value [2]. Atmospheric sensors can be inserted near power grids to obtain the localized information about the air quality. Vibration sensor and line sensors also help in condition monitoring [2]. However, wireless sensors are battery operated devices and it is expensive to change the battery periodically [3]. Despite the development in the field of battery technology the unpredictable lifetime of the batteries is of the major concern [4]. The power consumed by the sensor depends on the frequency at which the data is collected and communicated [5]. From the literature survey the low power sensor consumes around  $500\mu\text{W}$ - $1\text{mW}$ . To overcome this drawback, energy harvesting techniques is implemented to make sensors self-sustainable. The multiple energy sources in the power grid are solar, wind, vibration, electromagnetic field, electric field [3] and RF energy [6], [7]. The sources used should be independent of climatic conditions and should not be time variant [5]. As the sensors are used in power grids and are placed near high voltage devices for monitoring, electromagnetic field act as a major source for energy harvesting.

Electromagnetic field harvesters are broadly classified as clamped and non-clamped. A clamped magnetic harvester encloses the power line. This introduces line sag and also has the high maintenance risk. Non-clamped harvesters on other hand can be placed anywhere near the high voltage devices and hence are more flexible when compared to clamped harvester. As the harvester does not enclose the power line, harvested power is less when compared to clamped harvester [8]. N M Roscoe et al. [9] designed cast iron core with Radius 1.2cm and length 60cm to harvest electromagnetic field around high voltage devices. The device harvested 1mW of output power when placed in the flux density of  $4.5\mu\text{T}$ rms. Nina M Roscoe et al. [3] proposed optimum iron cast cylindrical core that delivers output power of  $300\mu\text{W}$  when placed in a electromagnetic field of  $18\mu\text{T}$ rms. The cylindrical core has a length of 50cm and diameter of 5cm. The core proposed in [9], [3] suffers from Foucault current (Eddy current) losses as the core is made of cast iron and also the length is high. Sheng Yuan et al. [10] propose bow tie ferrite core. The length is 15cm and diameter is 2cm. The harvester delivers  $360\mu\text{W}$  to the load when placed in magnetic flux density of  $7\mu\text{T}$ rms. Sheng Yuan et al. [11] propose helical core made of ferrite material. The core length is 15cm and has a diameter of 6cm. The core produces output power of  $612\mu\text{W}$  when placed in the flux density of  $7\mu\text{T}$ rms. However, the proposed helical core is difficult to manufacture in one piece, hence the core is

<sup>1</sup>\*Pavana H: Reva University, Bengaluru, Karnataka, School of Electronics & Communication Engineering

<sup>2</sup> Rohini Deshpande: Reva University, Bengaluru, Karnataka, School of Electronics & Communication Engineering

made of three parts and later joined together. This introduces air gap in the system, which lead to power loss. The core proposed here is efficient and simple to construct. The flux linkage is increased by connecting magnetic plate at end of the rod. The magnetic plate increases the flux density inside the core and hence more power can be harvested and delivered to the load. Section II discusses magnetic flux density in power stations, Section III deals with energy harvester design. Section IV discusses voltage doubler and energy management unit and section V, VI gives result and discussion and conclusion respectively.

## II. SOURCES OF MAGNETIC FIELD IN POWER GRID

Over head transmission lines and busbar in substation are found to be the main source of electromagnetic field energy. The other sources include transformers, ripple control systems and switch gear. J. Isokorpi et al. [12] propose that in power systems the major source of magnetic flux density are transmission lines, distribution lines, transformers and switching station. The maximum field in 400kV switching station is  $9.1\mu\text{T}_{\text{rms}}$ . In 110/20kV switching substations the maximum value of the field is  $18.6\mu\text{T}$  when measured at the height of 1m and  $14.8\mu\text{T}$  at 0.5m. T. Keikko et al. [13] Conclude that the highest electromagnetic field was caused by crossing of bus bar and outgoing feeder, 20kV cable from transformer to 20kV switch gear. The value is around  $18.6\mu\text{T}$  at a height of 1m and  $14.8\mu\text{T}$  at a height of 0.5m. Maja Grbic et al. [14] measure the electric and electromagnetic field intensity around 110kV/10kV substations around power transformers, 10kV busbar and power lines. The maximum magnetic flux density measured from 1.7m above the ground is  $86.15\mu\text{T.S}$ . Ozen et al. [15] find the electromagnetic field intensity around a transformer substations present in a hospital building which has high capacity transformers. The transformer here is 31.5kV/04kV. Field intensity across the transformer room is  $4.67\mu\text{T}$  and field intensity across control room is between  $1.74\mu\text{T}$  to  $27\mu\text{T}$ . The field is measured 1.5m above ground level. M. N. Oltean et al. [16] proposes that the intensity of electromagnetic field depends on distance from the overhead lines or the devices and also the current flowing through it. The electromagnetic field is measured below 400kV overhead line. The electromagnetic field density measured at 0.65m is  $5.284\mu\text{T}$  and  $5.160\mu\text{T}$  at 1.25m above ground. Maja Grbic et al. [17] propose to measure the flux density in the apartment near Belgrade Siberia 110kV/35kV substation. The main sources of electromagnetic field density are bus bars of 110kV and 35kV near wall of the apartment and ripple control system. The highest magnetic flux density around the apartment is around  $12\mu\text{T}$ - $20\mu\text{T}$ . It can be concluded from the above literature survey that Busbars and transformers in the electrical substation are the main source of electromagnetic field density.

## III. HARVESTER DESIGN

Magnetic core, voltage doubler and Energy management unit are the main parts of harvester.

A. *Magnetic core consists of*

1. Core which guides the flux path
2. Coil where voltage is induced.

Fig.1 gives approximation of the harvester circuit,

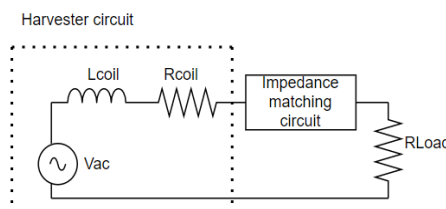


Fig.1 Harvester Circuit

$L_{\text{Coil}}$ =Inductance of the coil and  $R_{\text{total}}$  is total resistance offered by core material and copper coil

According to Faraday's law the voltage induced in a coil is given as below [3].  $f$  is Frequency of the electromagnetic field,  $\mu_E$  is effective permeability,  $r$  is the Radius,  $B$  is Magnetic Flux density and  $N$  is Number of turns.

$$V_{ac} = 2(\pi r)^2 f B N \mu_E \tag{1}$$

The power across the load

$$P_{out} = \frac{(V_{ac})^2}{4R} \tag{2}$$

The maximum power is transferred to load when the input impedance matches the output impedance according to maximum power transfer theorem. The value of  $R_{total}$  is equal to  $R_{Load}$ .

Output voltage generated across the load is half of the voltage generated in the coil.

$$P_{out} = \frac{V_{ac}}{2} \tag{3}$$

Power across load per unit volume is shown in (4)

$$volume = \pi r^2 l \tag{4}$$

$$P_{out} = \frac{(V_{ac})^2}{4R\pi r^2 l} \tag{5}$$

### B. Core Material

The main parameters of any magnetic core are the Relative permeability ( $\mu_r$ ) of the core, its electric conductivity, coercivity and saturation. Core with higher permeability gets strongly magnetized in response to the external electromagnetic field. The core material used here is ferrite Manganese-Zinc (Mn-Zn). Ferrites are soft magnetic cores. These cores have high permeability, low core losses, low electric conductivity and high electrical resistivity. High resistivity of ferrite reduces losses. Resistivity of ferrite Mn-Zn is in the order of  $1.1 \times 10^6 \Omega m$  [18,20].  $\mu_r$  of different core materials is listed in Table1. [19]

Table1. Relative permeability ( $\mu_r$ ) of different core materials.

Sl.No	Material	Relative Permeability
1	Iron(99.8%)	5000
2	Electrical steel	4000
3	Ferrite(MnZn)	2300
4	Ferrite(NiZn)	640
5	Permalloy	8000
6	Nanocrystalline	80000

Iron is also soft magnetic material. It presents high permeability and low resistivity. But iron has large Foucault current losses [18]. Nanocrystalline has very high permeability but has less resistivity when compared to ferrite; hence it is prone to more Foucault current losses [20]. The total loss in the harvester is due to core loss and copper loss. The core loss is due to alternating electromagnetic field. The core loss is made of Foucault current and hysteresis losses and copper loss is due to winding resistance of the coil [21].

The total resistance offered by the harvester is

$$R_{total} = R_{core} + R_{copper}$$

Core loss is made of two main components

- i. Hysteresis loss: Hysteresis losses depend on frequency and electromagnetic field. In this application both frequency and electromagnetic field is low hence hysteresis losses are ignored.
- ii. Foucault current loss: It is dependent on the electrical resistivity of the material. Power loss due to Foucault current is given as [22]

$$P_{eddy} = \frac{\pi^2 f^2 d^2 B^2}{16\rho} \tag{6}$$

Where  $d$  is the diameter,  $f$  is the frequency of the flux,  $B$  is electromagnetic flux density,  $\rho$  is the resistivity. The resistivity of the ferrite material is very high. The core designed here has smaller diameter, this result in low Foucault current losses and hence are also ignored. The core resistance is very small when compared to winding resistance and hence the total loss is due to the resistance offered by winding coil.

C. Core shape

The power harvested depends on of the magnetic core. Effective permeability ( $\mu_E$ ) is applicable to magnetic core with air gaps. The core in which the flux is not guided by magnetic material completely, they pass through air leading to  $\mu_E$ . It depends on the demagnetization factor. Whenever a cylindrical magnetic core is subjected to external electromagnetic field, a demagnetizing field is generated that cancels the applied electromagnetic field. Fig.2 shows the magnetization in cylindrical core

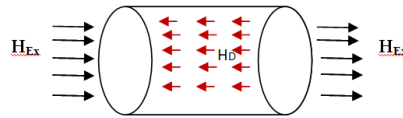


Fig.2 Magnetization of the core  $H_{ext}$ =Applied electromagnetic field ,  $H_D$ = Demagnetizing field

The relationship between the Effective permeability ( $\mu_E$ ) of the core and demagnetization factor is shown in (7)[23]

$$\mu_E = \frac{\mu_r}{1+N_d\mu_r} \tag{7}$$

$N_d$ =Demagnetization factor,  $\mu_r$  =Relative Permeability of the material. Demagnetization factor depends on length and diameter of the core and the core material. The  $\mu_E$  for different core shapes is calculated using (8 ) [23]

$$\mu_E = \frac{B_{in}}{B_x} \tag{8}$$

$\mu_E$  increases, with the increase in  $\mu_r$  of the core material for an optimized value of length to diameter ratio of the core [3]. After the certain value it becomes independent of  $\mu_r$  and will not provide any significant raise. Hence large value of  $\mu_r$  does not improve the harvested power. The Effective permeability of the ferrite core as function of length to diameter ratio is given in Fig.3.

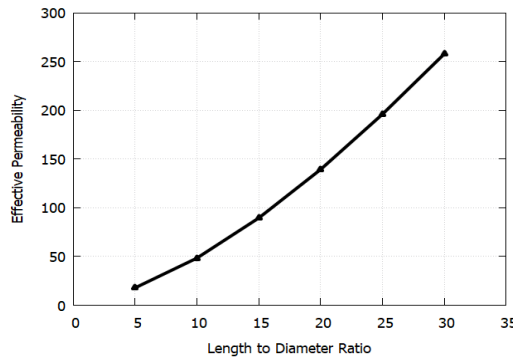


Fig.3 Effective permeability as a function of length to diameter ratio.

$\mu_E$  is proportional to length to diameter ratio of the magnetic core. The core with larger aspect ratio harvest more power. However they are fragile and are prone to damage. Hence aspect ratio of the core must be optimized. Let  $L$  be length of the core and  $D$  is diameter of the core. The aspect ratio of the core is given in (9)

$$\gamma=L/D \tag{9}$$

Demagnetization factor  $N_d$  is (10) [23]

$$N_d = \frac{1}{\gamma^2 - 1} \left[ \frac{\gamma}{\sqrt{\gamma^2 - 1}} \ln(\gamma + \sqrt{\gamma^2 - 1}) - 1 \right] \tag{10}$$

Relationship between demagnetization and aspect ratio is given in Fig.4. Long and thin core increases the distance between North Pole and South Pole and hence demagnetization decreases.

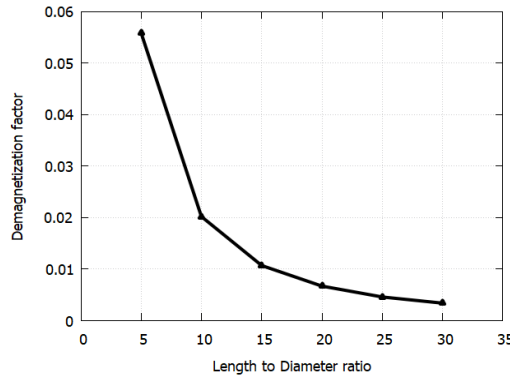


Fig.4 Demagnetization factor versus length to diameter ratio.

To find the optimized length to diameter ratio of the core, a cylindrical ferrite core as in Fig.5 is placed in the uniform electromagnetic field of 9μT generated using Helmholtz coil in CST EM Studio. The flux density linked to the core is measured.

$\mu_r = 2300$ ,  $N=200$  and magnetic flux density linked to the core is measure for different length to diameter ratio.  $L$  is the length of the core and  $D_{in}$  the diameter of the core.

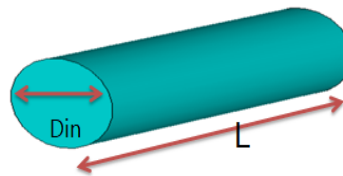


Fig.5 Cylindrical rod

The relationship between Effective permeability and Relative permeability is explained in Fig.6.  $\mu_E$  for different length to diameter is measured and plotted as the function of  $\mu_r$ . It increases, with the increase in Relative permeability of the core material up to a certain value and later it is independent of increase in  $\mu_r$ .

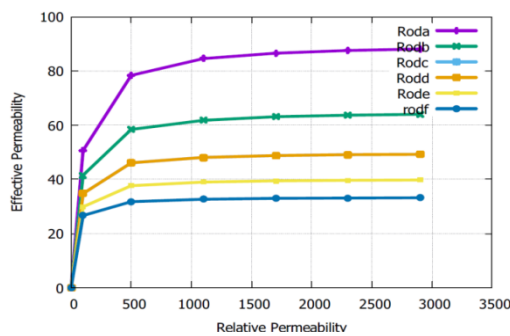


Fig.6 Effective Permeability as a function of Relative Permeability for different length to diameter ratio

{Rod(a)Din=2cm}, {Rod(b)Din=2.5cm}, {Rod(c)Din=3cm}, {Rod(d)Din=3.5cm}, {Rod(e)Din=4cm}, {Rod(f)Din=4.5cm}.

The simulated result for core with different length to diameter ratio is given in Table 2. The length of the core is kept constant by varying the diameter of the core. As the core diameter increases, the resistance of the coil resistance is increased. Core with larger turns, offers more coil resistance reducing the harvested power.

Table.2 Output power of the core for different diameter and when  $\mu_r=2300$ ,  $N=200$ ,  $L=25\text{cm}$ .  
 {Rod(a)Din=2cm},{Rod(b)Din=2.5cm},{Rod(c)Din=3cm},{Rod(d)Din=3.5cm},  
 {Rod(e)Din=4cm},{Rod(f)Din=4.5cm}.

Core	$\mu_E$	$N_d$	$V_{Coil}$ (mV)	$V_o$ (mV)	$R_{Coil}$ ( $\Omega$ )	$P_{Out}$ ( $\mu W$ )
Rod(a)	87.1	0.011	15	7.5	4.4	13.5
Rod(b)	63.3	0.016	17.5	8.7	5.5	13.9
Rod(c)	48.7	0.020	19.4	9.7	6.6	14.3
Rod(d)	39.3	0.026	21.3	10.6	7.7	14.7
Rod(e)	32.8	0.031	23.3	11.6	8.8	15.4
Rod(f)	28.1	0.036	25.2	12.6	9.9	16

D. Design of Dumbbell core

Flux linkage to the core increases with the increase in length to diameter ratio of the magnetic core. Long and thin core are very brittle and there is a likelihood of breaking. Hence the aspect ratio of the core must be optimized. The flux linkage of the core is increased without further increasing the length to diameter ratio by attaching the magnetic plate on either side of the core. This result in the dumbbell shaped core.

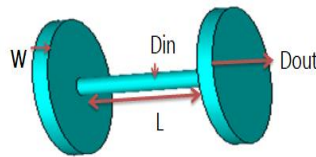


Fig.7 Dumbbell core

$D_{in}$  is the inner diameter of the core,  $D_{out}$  is the outer diameter,  $L$  is the length and  $W$  is the width of the magnetic plate. Dumbbell shaped core with  $D_{in}=2\text{cm}$ ,  $L=25\text{cm}$ ,  $W=2.6\text{cm}$  is designed and simulated by varying the diameter of the magnetic plate and keeping its width constant.  $N=200$  and  $\mu_r =2300$ . Simulated results are tabulated in Table 3. There is a significant rise in the output power when the diameter of the magnetic plate increases. From Table 2 and Table 3 it is noticed that the output power harvested by the cylindrical rod is  $13.5\mu W$  when  $D_{in}=2\text{cm}$ ,  $\mu_r=2300$ ,  $N=200$ ,  $L=25\text{cm}$  whereas, dumbbell shaped core with  $D_{out}=14\text{cm}$  harvests  $193\mu W$ .

Table 3. Output power of the cores for different diameter and when  $\mu_r=2300$ ,  $N=200$ ,  $L=25\text{cm}$ .  
 {Rod(a)Dout=10cm},{Rod(b)Dout=12cm},{Rod(c)Dout=14cm},{Rod(d)Dout=16cm},  
 {Rod(e)Dout=18cm},{Rod(f)Dout=20cm}.

Core	$\mu_E$	$N_d$	$V_{coil}$ (mV)	$V_o$ (mV)	$R_{Coil}$ ( $\Omega$ )	$P_{Out}$ ( $\mu W$ )
Rod(a)	251.1	0.003	44.6	22.3	4.4	112.5
Rod(b)	290.6	0.003	51.6	25.8	4.4	150.8
Rod(c)	328.8	0.003	58.4	29.2	4.4	193.0
Rod(d)	367.7	0.002	65.3	32.6	4.4	241.4
Rod(e)	407.7	0.002	72.4	36.2	4.4	296.8
Rod(f)	477.7	0.002	84.8	42.3	4.4	407.4

Dumbbell shaped core is placed in the uniform electromagnetic field of  $9\mu\text{T}$  generated using Helmholtz coil in CST EM Studio to optimize the aspect ratio of the core. Table 4 has simulated output power for dumbbell core with  $D_{in}=2\text{cm}$ ,  $L=25\text{cm}$ ,  $N=200$  and  $\mu_r = 2300$ . The magnetic plate diameter  $D_{out}=11\text{cm}$  and the width of the outer plate  $W$  is varied.

Table 4. Parameters of the cores for different diameter and when  $\mu_r=2300$ ,  $N=200$ .  $W$  is varied.

{Rod(a) $W=2\text{cm}$ }, {Rod(b) $W=2.5$ }, {Rod(c) $W=3\text{cm}$ }, {Rod(d) $W=3.5$ }, {Rod(e)  $W=4$ }, {Rod(f)  $W=4.5$ }

Core	$\mu_E$	$N_d$	$V_{coil}$ (mV)	$V_o$ (mV)	$R_{Coil}$ ( $\Omega$ )	$P_{Out}$ ( $\mu\text{W}$ )
Rod(a)	253.3	0.003	45	22.5	4.4	114.5
Rod(b)	265.5	0.0037	47.1	23.5	4.4	125.7
Rod(c)	278.8	0.0036	49.5	24.7	4.4	138.8
Rod(d)	298.8	0.0035	53	26.5	4.4	159.4
Rod(e)	303.3	0.0033	53.8	26.9	4.4	164.1
Rod(f)	316.6	0.0031	56.2	28.1	4.4	178.9

It can be seen from Table 4 that output power increases with the increase in the width of the magnetic plate. Fig.8 gives the output power as a function of diameter of the magnetic plate.

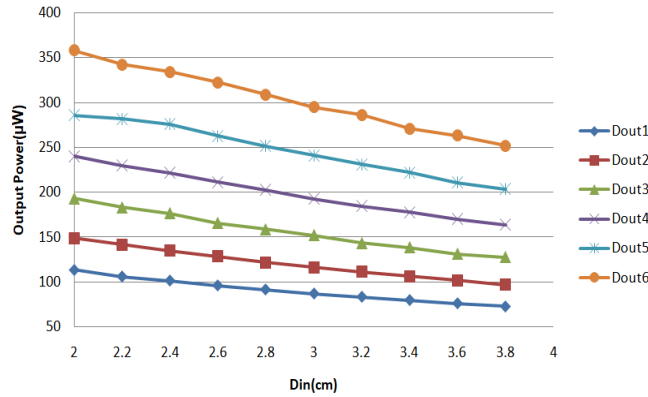


Fig.8 Output power as a function of diameter of the magnetic plate

Maximum power is harvested when dumbbell core has thin and long inner rod and larger magnetic plate. Thin and long inner rod makes the core brittle. And increase in outer diameter of the dumbbell core increases the core volume. Fig.9 and Fig.10 compares flux density inside the cylindrical rod and dumbbell core. The cores are placed in the external electromagnetic field of  $9\mu\text{T}_{rms}$ .

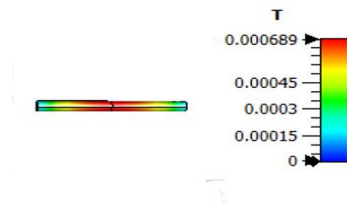


Fig.9. Magnetic flux density inside the cylindrical rod

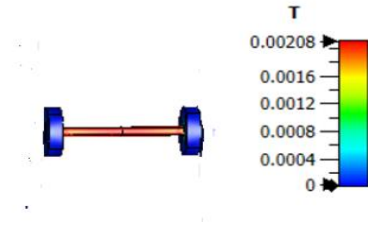


Fig.10 Magnetic flux density inside the dumbbell core

The cylindrical rod is simulated with diameter  $D_{in}=2.2\text{cm}$  and length  $L=25\text{cm}$ . The flux density in the middle of the core is  $689\mu\text{Trms}$ . Dumbbell core is simulated with  $D_{in}=2.2\text{cm}$ ,  $D_{out}=11\text{cm}$ ,  $W=2.8\text{cm}$  and length  $L=25\text{cm}$ . The flux density in the middle of the core is  $2.08\text{mTrms}$ . Magnetic plate across the cylindrical rod increases flux linkage. The dumbbell core with inner diameter  $D_{in}=2.2\text{cm}$ ,  $L=25\text{cm}$  and magnetic plates with diameter  $D_{out}=11\text{cm}$  and width  $W=2.8\text{cm}$  is proposed in the present work.

*E. Coil Design*

The voltage from the harvester also depends on the copper coil wounded on the core. It is directly proportional to number of turns. Increase in the number of turn  $N$  increases the coil resistance. Total resistance of the harvester consists of core resistance and resistance of the coil wounded on the core. Coil resistance cause copper losses and core resistance cause Foucault current and hysteresis loss. Foucault current and hysteresis loss becomes negligible as the material selected is ferrite. Ferrite (Mn-Zn) has less electric conductivity and the frequency of operation is  $50\text{Hz}$ . Hence only copper loss is considered. Properties of the copper coil are investigated below. Fig.11 is copper coil resistance as a function of number of turns for different core diameter. It can be seen from Fig.11 that, as the number of turns increases, the coil resistance increases. The core with greater inner diameter offers more resistance for a given number of turns.

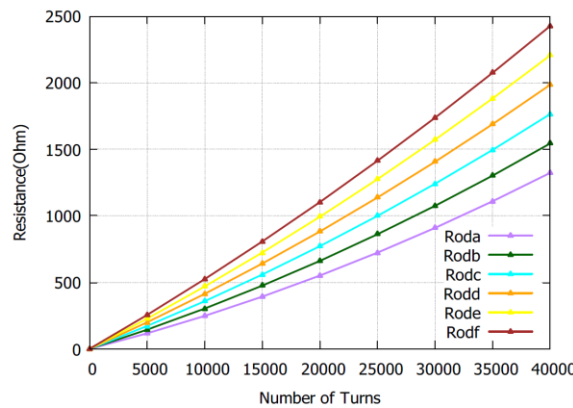


Fig.11 Coil Resistance as a function of Number of turns

The total wire length is given by [24]

$$L_{\text{wire}} = 2\pi N (D + (J_{\text{Layer}} * d)) \tag{11}$$

Where  $N$  is the number of turns in the coil,  $d$  is the diameter of the wire,  $D$  is the diameter of the core,  $J_{\text{Layer}}$  is number of layers wounded.

$$J_{\text{Layer}} = \frac{N}{(W/d)} \tag{12}$$

$W$  is width of copper coil. The diameter of the copper coil wounded on the core is also an important parameter. Fig.12 gives the relationship between wire diameter and resistance for different coil turns. The wire with larger diameter has less resistance but they occupy larger area in the core and hence reduce the number of turns.



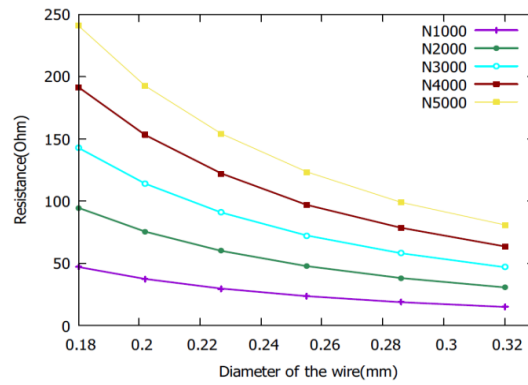


Fig.12 Resistance of the coil when different wires are used

Number of turns is directly proportional to output voltage. Fig.13 explains the number of turns as the function of wire diameter. When wire diameter increases, number of turns reduces. This is because with the increase in the wire diameter the area occupied by the wire on the core increases. This results in less number of turns.

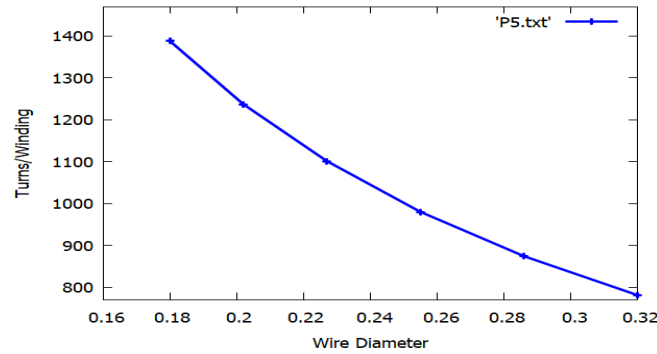


Fig.13 Number of turns/winding as the function of wire diameter.

The relationship between output power as the function of AWG is given in Fig.14. American Wire Gauge (AWG) is standard measure for the diameter of electrical conductors. In American Wire Gauge, larger the value, smaller the wire thickness and diameter. From Fig. 14 it can be seen that as the AWG increases, the output power increases. This is because larger the value of AWG smaller the diameter. The wire with the smaller diameter occupies less area and hence more number of turns. The wire chosen her is with diameter 0.255mm and resistivity of 0.352Ω/m.

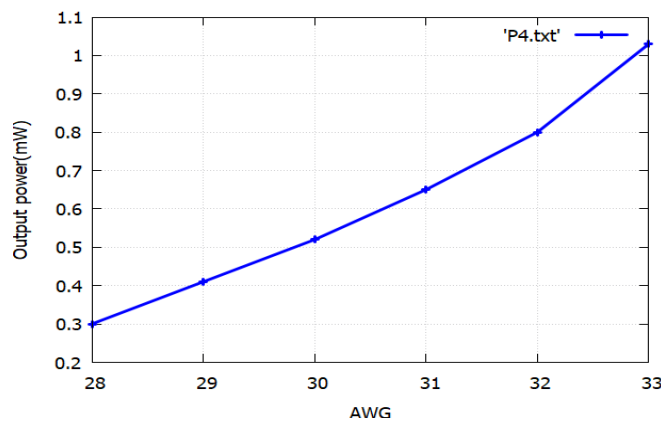


Fig.14 Output power as the function of AWG

#### IV. ENERGY MANAGEMENT UNIT

The output from the magnetic coil must be rectified and regulated and then sent to sensors. Voltage doubler and energy management unit is designed to obtain constant voltage. It is essential to implement voltage doubler in harvester because; the output from magnetic core is low. The voltage doubler consists of 2 diodes and 2 capacitors. Schottky diode is used due its low voltage drop, low conduction loss and small reverse current [26]. The Schottky diode PMEG2020AEA with forward voltage drop of 0.19V is used. L shaped impedance matching circuit is designed to obtain maximum efficiency [27].The output from voltage doubler is applied to energy management to obtain regulated voltage.

The energy management unit consists of

1. Over voltage protection circuit
2. Under voltage lockout circuit
3. Linear regulator

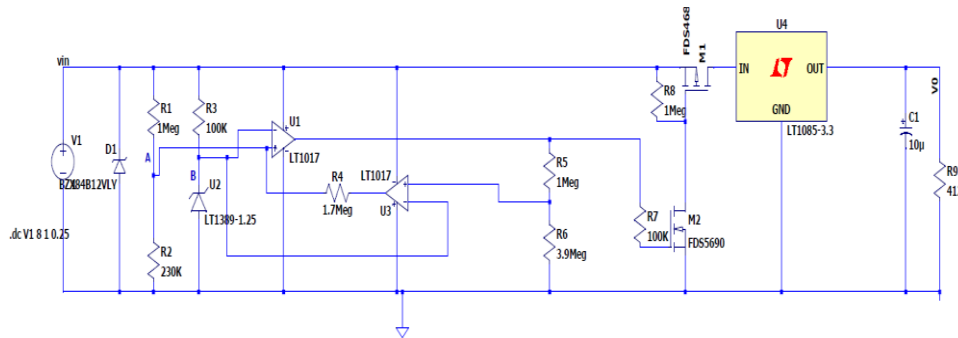


Fig.19 Energy management unit

Fig.19 is the energy management unit designed to obtain the regulated output. Zener diode is used as over voltage protection. This circuit avoids low power devices getting damaged due to over voltage. BZX84C12VLzener diode is used here. It has reverse breakdown voltage of 12V and has reverse leakage current of 0.1µA. Under voltage lockout circuit is designed to monitor voltage provided to the sensors. It ensures sensors are isolated from the harvester until a threshold voltage is reached. In the UVLO circuit Zener diode LT1389 is used to provide the reference voltage across inverting terminal of the comparator. The reference voltage provided is 1.25V. This diode requires only 800nA current to operate. Resistor R1,R2 and R5, R6 provides divided input voltage to non-inverting terminal of the comparator.R3, R4 is a current limiting resistor.R7 and R8 is used to reduce the noise in the switching of MOSFETS. The comparator used here is LT1017. It is a very low supply comparator. The supply current is just 15nA. The voltage range is from 1.1V to 40V.P Channel MOSFET and N channel MOSFET used here is FDS4685 and FDS5690 respectively. FDS4685 is P channel MOSFET with high switching speed and a very low RDS(on). RDS(on) is between 0.027Ω to 0.035Ω. It has very low leakage current of 1µA.FDS5690 is N channel MOSFET is used for application which requires fast switching speed and low loss. It has RDS(on) is between 0.028Ω to 0.033Ω. It has high power and current handling capability. It has very low leakage current of 1µA.The Wireless sensors considered here is MICAZ MPR2400. This sensor needs supply voltage of 3.3V, average current 8mA and power consumption of 27mW. Output from UVLO circuit is passed to linear regulator. Linear Regulator is used to maintain steady voltage. It is used to provide stable output to the wireless sensor. The regulator used here is LT1083-3.3. It provides regulation for a range of 4.8V to 15V. The regulated output obtained is 3.3V.

#### V. RESULTS AND DISCUSSION

Uniform Electromagnetic field can be generated using Helmholtz coil. Helmholtz coil is shown in Fig.15 [25]

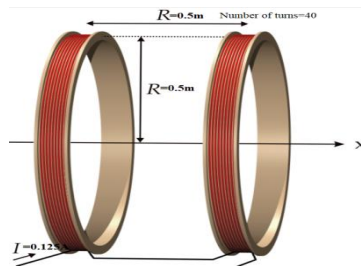


Fig. 15 Helmholtz coil

Here R is the Radius of the coil, in meters. Helmholtz has two magnetic coils that are identical to each other separated by the distance R, which is equal to the Radius of the coil. Electromagnetic flux density (B) generated by Helmholtz coil is calculated in (13) [25]

$$B = \frac{\mu_0 8NI}{R\sqrt{125}} \tag{13}$$

$\mu_0$ =permeability of free space, N =number of turns wounded on the Helmholtz coil. I is current through the coil, in amperes. In this experiment, the Radius of each coil is 0.5m and the N used here is 40. The current through each coil is 125mA. The distance between two coils is 0.5m. The generated flux is 9 $\mu$ T. A Cylindrical ferrite rod with  $\mu_r =2300$  is used as the core material. The coil used has a diameter 0.255mm and resistivity of 0.352 $\Omega$ /m. Fig.16 gives output power as function of number of turns in cylindrical rod.

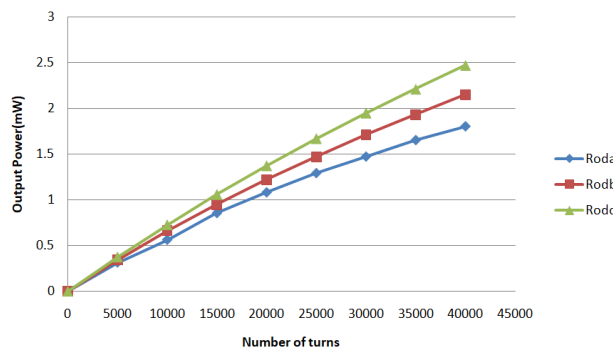


Fig. 16 Output power as function of coil turns in cylindrical rod.

{Rod(a)Din=2cm},{Rod(b)Din=3cm},{Rod(c)Din=4cm}, L=25cm,  $\mu_r=2300$

To increase the electromagnetic flux density in the ferrite core, magnetic plates are added across the cylindrical rod and are simulated for different values of cylindrical rod diameter and number of turns. The diameter of the magnetic plates and width are kept constant. Fig.17 gives output power as function of number of turns.

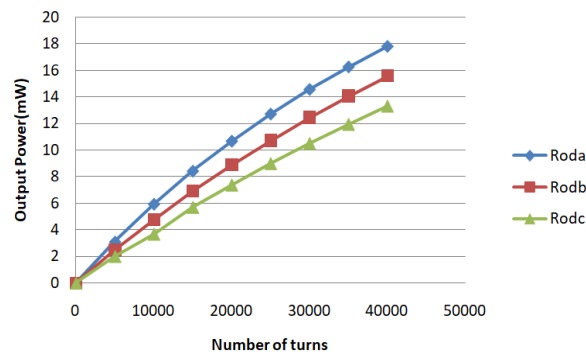


Fig. 17 Output power as function of number of turns in dumbbell core.

{Rod(a),Din=2cm},{Rod(b)Din=3cm},{Rod(c)Din=3cm},D<sub>out</sub>=1.1cm, W=2.8cm is kept constant

The output power from dumbbell core is much larger than the cylindrical rod as the magnetic plate increases the flux linkage. The proposed dumbbell core is designed and simulated using CST EM Studio. Dumbbell Core with Inner diameter  $D_{in}=2.2\text{cm}$ , Length= $25\text{cm}$  and  $D_{out}=11\text{cm}$  and width  $W=2.8\text{cm}$  is designed and simulated in the flux density of  $9\mu\text{T}$ . Wire diameter  $0.255\text{mm}$  and resistivity of  $0.352\Omega/\text{m}$  is considered. The power for different number of turns is plotted. Table 5 gives the output power for different number of turns.

Table 5. Simulated output for multiple number of turns.

Number of turns	Open circuit voltage	Output Power
200	49mV	0.12mW
2000	499mV	1.25mW
20000	4.99V	10mW
40000	9.98V	17.63mW

Output power for different number of turns is given in Fig.18.

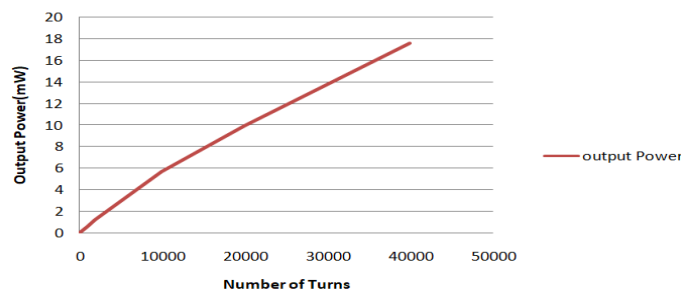


Fig. 18 The power for different number of turns is plotted.

The output power harvested for the proposed core is  $1.25\text{mW}$  and power density is  $1.99\mu\text{W}/\text{cm}^3$  for 2000 number of turns. As the number of turns is increased the output power increases. The length of the core is  $25\text{cm}$ , its inner diameter is  $2.2\text{cm}$  and diameter of magnetic plate is  $11\text{cm}$  and width of the plate is  $2.8\text{cm}$ . If the harvester is placed near higher flux density, more power can be harvested. The Table 6 gives the comparison between various previous designs.

Table 6. Comparison with previous design

Parameters	Solenoid [3]	Bowtie [10]	Helical[11]	Dumbbell core
Flux density( $\mu\text{T}_{rms}$ )	18	7	7	9
Length(cm)	50	15	15	25
The Number of turns	40,000	40,000	400	2,000
The wire diameter(mm)	-	0.14	0.4	0.255
Output power (mW)	0.3	0.25	0.6	1.25
Volume( $\text{cm}^3$ )	981	188	292	627

## VI. CONCLUSION

Dumbbell shaped core is designed to harvest electromagnetic field near voltage devices in electrical substation. The proposed core is not clamped on transmission line and can be placed near high voltage devices. It has magnetic plate connected to the cylindrical rod that increases the flux linkage and hence increases the harvested power. The core designed here is simple in construction when compared to the previous design. From the results it is shown that the output power density of the dumbbell core with 2000 turns is  $1.99\mu\text{W}/\text{cm}^3$  and is enough to power any low power sensors. Output power can be further increased by increasing the number of turns on the

core. Voltage regulator and energy management unit is designed to obtain steady state output to sensor and making them self-sustainable.

#### ACKNOWLEDGMENT

Authors acknowledge the support from REVA University for the facilities provided to carry out the research.

#### REFERENCES

- [1] Oktay Cetinkaya, Ozgur B. Akan "Electric-Field Energy Harvesting in Wireless Networks" IEEE Wireless Communications Vol.24, Iss.2, pp.34-41 April 2017.
- [2] Z Wu, D S Nguyen, R M White "Electromagnetic energy harvester for atmospheric sensor on overhead power distribution lines" IOP conf. series Journal of physics 2018.
- [3] Nina M Roscoe, Martin D. Judd "Harvesting Energy from Electromagnetic fields to Power Condition Monitoring Sensors" IEEE Sensors Journal, Vol.13, June 2013.
- [4] Shen Guo, Peng Wang, Jichuan Lin "Power harvesting technologies in the power grid" 2018 China International conference on electricity distribution 17-19 September 2018.
- [5] M Zhu, M D. Judd, P.J Moore, R Zhang "Energy Harvesting Techniques for Powering Autonomous Sensors within Substations" 2009 International Conference on Sustainable Power Generation and Supply 6-7 April 2009.
- [6] Kunwar Pal Singh, Rohini Deshpande "UWB Spiral Antenna with Balun for EM Energy Harvesting" RAUS-SASTech Journal Vol.Iss.16 pp1-4 2017.
- [7] K.P Singh, Rohini Deshpande, "Energy Harvesting from Electromagnetic interference and Jamming Signals in Radar System – Survey" International Conference on Emerging Trends in Engineering and Technology, Bengaluru, India, July 4th – 5th 2015
- [8] Pavana H, Dr. Rohini Deshpande "Energy Harvesting Techniques for Monitoring Devices in Smart Grid Application" 2020 Third International Conference on Advances in Electronics, Computers and Communications (ICAIECC) 11-12 December 2020.
- [9] N M Roscoe, M D Judd, I Fraser "A Novel Inductive Electromagnetic Energy Harvester for condition Monitoring Sensors." CMD2010, 2010
- [10] Sheng Yuan, Yi Huang "Electromagnetic field energy harvesting under overhead power lines," IEEE Trans. Power Electron. Vol.30, Iss. 11, November 2015
- [11] Sheng Yuan, Yi Huang, Jiafengzhou "A High-Efficiency Helical Core for Electromagnetic field Energy Harvesting" IEEE Transactions on Power Electronics, Vol.32, Iss.7, pp 5365-5376 July 2017.
- [12] J. Isokorpi, T. Keikko, L. Korpinen "Power frequency electric and electromagnetic fields at a 110/20 kV substation" PowerTech Budapest IEEE conference 06 August 2002
- [13] T. Keikko, S. Kuusiluoma, T. Sauramaki, L. Korpinen "Comparison of electric and electromagnetic fields near 400 kV electric substation with exposure recommendations of the European Union" IEEE/PES Transmission and Distribution Conference and Exhibition 6-10 Oct. 2002.
- [14] Maja Grbic, Aleksandar Pavlovic, Dejan Hrvic "Levels of electric and electromagnetic fields inside 110/x kV substation" IET journal June 2017.
- [15] S. Ozen, H. F. Carlak, O. H. Colak, S. Helhel "Electromagnetic field risk analysis for employees and patients due to power transformers in hospital buildings" 2017 Progress In Electromagnetics Research Symposium - Spring (PIERS) IEEE 22-25 May 2017

- [16] M. N. Oltean, T. Fagarasan, G. Florea, C. Munteanu, A. Pop “Electroelectromagnetic field measurement on high voltage overhead lines” 2017 12th International Conference on Live Maintenance (ICOLIM) 26-28 April 2017.
- [17] Maja Grbić, Aldo Canova, Luca Giaccone “Levels of electromagnetic field in an apartment near 110/35 KV substation and proposal of mitigation techniques” Mediterranean Conference on Power Generation, Transmission, Distribution and Energy Conversion (MedPower 2016) 6-9 Nov. 2016.
- [18] D.A Vieira, Cleonilson, Yuri P Molina “Energy harvesting using magnetic induction considering different core materials” IEEE Instrumentation and measurement technology conference may 2014.
- [19] Engineering ToolBox, (2016). Permeability. [online] Available at: [https://www.engineeringtoolbox.com/permeability-d\\_1923.html](https://www.engineeringtoolbox.com/permeability-d_1923.html) 30-06-2021
- [20] ByteMark(2011)[online] Available at [http://www.bytemark.com/products/Nanocrystalline\\_cores.html](http://www.bytemark.com/products/Nanocrystalline_cores.html) 20-8-2021
- [21] Vishay Intertechnology INC [online] “Inductors Instructional guide” Available: <https://www.vishay.com/docs/49782/49782.pdf> 20-8-2021
- [22] Asbjorn Engmark Espe, Geir Mathisen “Towards electromagnetic field energy harvesting near electrified railway tracks” 2020 9th Mediterranean conference on embedded computing, 8-11 June 2020.
- [23] Kuniyoshi Tashiro, Hiroyuki Wakiwaka, Gen-Ya Hattori “Estimation of effective permeability of dumbbell-shaped magnetic core” IEEE Transactions on magnetic, vol.51, iss.1, January 2015.
- [24] M.E kiziroglou, S.W. Wright, E.M. Yeatman “Coil and core design for inductive energy receivers” Sensors and Actuators A: Physical Elsevier, 13 July 2020.
- [25] M. Saqib, F. S. N. and F. J. N., "Design and Development of Helmholtz Coils for Electromagnetic field ," 2020 International Youth Conference on Radio Electronics, Electrical and Power Engineering
- [26] T. Sathiyapriya, V Gurunathan, K N Krishna Prasad, T Naveen Kumar “Voltage Doubler Design for RF Energy Harvesting System” IEEE 7th International Conference on Smart Structures and Systems ICSSS 2020 (EEPE), 2020, pp. 1-5.
- [27] Shiquan Fan, Wei Gou, Yang Zhao “A 2.45-GHz Rectifier-Booster Regulator With Impedance Matching Converters for Wireless Energy Harvesting” IEEE Transactions on microwave theory and techniques, Vol.67, No.9, Sept.2019.